JOURNAL OF CATALYSIS **161,** 198–205 (1996)
ARTICLE NO. 0177

Catalytic Properties of Iron Phosphate-Based Catalysts Containing $Fe_2(PO_3OH)P_2O_7$ and α- or β-$Fe_3(P_2O_7)_2$ in the Oxidative Dehydrogenation of Isobutyric Acid

P. Bonnet and J. M. M. Millet[1]

Institut de Recherches sur la Catalyse, CNRS, associé a l'Université Claude-Bernard, Lyon I, 2 avenue Albert Einstein, F-69626 Villeurbanne Cedex, France

Received June 27, 1995; revised January 22, 1996; accepted January 30, 1996

The formation of β- and α-$Fe_3(P_2O_7)_2$ along with $Fe_2(PO_3OH)P_2O_7$, in iron phosphate-based catalysts for oxidative dehydrogenation of isobutyric acid, has been studied by Mössbauer spectroscopy and X-ray diffraction. It has been shown that the crystallization of β-$Fe_3(P_2O_7)_2$ in the catalysts under the conditions of catalysis is related to the presence in the amorphous precursors of these catalysts of particular ferrous species, whereas the crystallization of α-$Fe_3(P_2O_7)_2$ occurred when the catalysts were tested under low oxygen partial pressure. From a catalytic point of view, the β-$Fe_3(P_2O_7)_2$ phase appeared to be poorly active and selective and without effect on the catalytic properties of $Fe_2(PO_3OH)P_2O_7$. On the contrary, the high activity and selectivity of α-$Fe_3(P_2O_7)_2$ were confirmed. Comparison of the catalytic properties of catalysts containing the same amount of β-$Fe_3(P_2O_7)_2$ along with a large proportion of α-$Fe_3(P_2O_7)_2$ or $Fe_2(PO_3OH)P_2O_7$ clearly showed that the catalytic properties of these two last phases were very close. This last feature has been proposed to be correlated with the presence at the surface of both phases under the conditions of catalysis of the same species [$(PO_3OH)^{2-}$ and $(Fe_3O_{12})^{16-}$ or $(Fe_2O_9)^{13-}$ groups].

1. INTRODUCTION

The oxidative dehydrogenation of isobutyric acid (IBA) is an alternative way to obtain methacrylic acid (MAA) and, in the future, could be used in a new industrial process for production of methylmethacrylate. Several patents claim the use of iron phosphate-based catalysts for this reaction (1–3). A new process for preparation of these catalysts has been developed in our laboratory (4). This process consists of reacting vivianite with pyrophosphoric acid under reflux in acetone; this leads to amorphous precursors which are transformed under the conditions of catalysis into a new phase, $Fe_2(PO_3OH)P_2O_7$ (4). This phase is as selective as the industrial catalysts prepared as described in the patents but approximately five times more active. The catalytic properties have been proposed to be related to the formation of an amorphous phase over 5 nm around the $Fe_2(PO_3OH)P_2O_7$ particles (4).

It was observed that depending on the conditions of synthesis of the precursors or on their catalytic activation conditions, the precursors could be transformed not only into $Fe_2(PO_3OH)P_2O_7$, but also into two other phases: α- and β-$Fe_3(P_2O_7)_2$. The phase α-$Fe_3(P_2O_7)_2$ was identified some years ago as the active and selective phase of several iron phosphate-based catalysts (5–7). β-$Fe_3(P_2O_7)_2$ is a high-temperature form (8). It has recently been identified in iron phosphate-based catalysts by Muneyama *et al.*, who referred to it as phase B (9, 10).

The aim of this work was to investigate in more detail the conditions leading to the formation of phases α- and β-$Fe_3(P_2O_7)_2$ in the catalysts after activation and their influence on the catalytic properties. For this purpose, precursors with different oxidation levels have been prepared along with pure β-$Fe_3(P_2O_7)_2$ and tested as catalysts under different conditions. All the catalysts tested were characterized before and after catalytic runs by Mössbauer spectroscopy and X-ray diffraction.

2. EXPERIMENTAL

2.1. Preparation of Catalyst Precursors

Iron phosphate catalyst precursors have been synthesized by reacting, under reflux, vivianite, a hydrated ferrous iron phosphate $Fe_3(PO_4)_2 \cdot 8H_2O$, and $H_4P_2O_7$ in acetone. The reaction was carried out for 15 h in a 250-ml flask equipped with a mechanical stirrer and reflux condenser. The reactant P/Fe ratio was set equal to 4.5 by use of the appropriate amount of pyrophosphoric acid. After completion of the reaction, the solid phases were recovered by filtration, washed with acetone, and dried at 313 K in air. Solids were synthesized under different rates of refluxing obtained by varying the temperature of the heating source between 308 and 573 K. β-$Fe_3(P_2O_7)_2$ was prepared

[1] To whom correspondence should be addressed. Fax: 33-72445399.

0021-9517/96 $18.00

by the solid-state reaction of $Fe_2P_2O_7$ and $Fe_4(P_2O_7)_3$ at 1173 K under vacuum (4). $Fe_2P_2O_7$ was obtained by reduction of $FePO_4$ at 1023 K in an N_2–H_2–H_2O mixture (11), and $Fe_4(P_2O_7)_3$ was prepared by heating ferric nitrate and diammonium hydrogen phosphate up to 1123 K. The synthesized precursors, designated P, have all been shown to be partially reduced. Their $Fe^{2+}/(Fe^{2+} + Fe^{3+})$ was determined and is expressed, for example, as P6 for a precursor with a $Fe^{2+}/(Fe^{2+} + Fe^{3+})$ ratio of 6. Once this precursor has been tested as a catalyst, it would be denoted C6. Another precursor has been prepared as described with a heating source temperature of 308 K but with as starting reactant a vivianite sample dehydrated by heating for 2 h at 573 K under nitrogen; it is referred to as PD and, after catalysis, as CD.

2.2. Analytical Methods

Powder X-ray diffraction patterns were obtained using a Siemens D500 diffractometer and Cu$K\alpha$ radiation. The iron and phosphorus contents were quantitatively determined by atomic absorption and the specific surface areas by the BET method using nitrogen adsorption. ^{57}Fe Mössbauer spectroscopy was performed at 298 K as previously described using ^{57}Co as a radiation source (12). The samples were diluted in Al_2O_3 to avoid a too high Mössbauer adsorption and pressed into pellets. The isomer shifts are given with respect to α-Fe. The relative areas of the observed doublets have been used to evaluate quantitatively the relative ratios of the phases present in the catalysts. This has been done by assuming equal free recoil fraction for all the sites. The validity of the computed fits was judged on the basis of both χ^2 values and convergence of the fitting processes.

2.3. Catalytic Test Procedures

The oxidative dehydrogenation of isobutyric acid to methacrylic acid was carried out at atmospheric pressure in a dynamic differential microreactor. Standard conditions were as follows: total flow rate, 1 cm^3 s^{-1}; reaction temperature, 658 K; O_2/IBA/H_2O/N_2, 4.26/5.86/72.0/19.2 kPa. The samples were tested with a mass of 30 to 50 mg at a comparable low conversion level of approximatively 20%. Propene, acetone, and CO_2 were the three by-products formed with methacrylic acid (13, 14). All the catalysts were recovered after testing under the conditions given above except C14 and C26, which were used to study the influence of oxygen partial pressure on catalytic performance and recovered after catalytic tests performed with oxygen partial pressures equal to 1.32 and 2.63 kPa, respectively (4).

3. RESULTS AND DISCUSSION

3.1. Characterization of the Catalysts before and after Catalytic Tests

Seven precursors were prepared using different refluxing rates. We have previously shown that this parameter determined the extent of oxidation of the amorphous precursors (4). The main characteristics of the precursors prepared and studied are presented in Table 1. Their $Fe^{2+}/(Fe^{3+} + Fe^{2+})$ ratios were calculated from Mössbauer spectroscopic data. The P/Fe ratios of all the amorphous precursors were approximately the same and their surface areas were similar, ranging from 1.3 to 2.2 m^2 g^{-1}.

TABLE 1

Physicochemical Characteristics of the Prepared Compounds

Compound	P/Fe	S_{BET} (m^2 g^{-1})	$Fe^{2+}/(Fe^{3+} + Fe^{2+})$
P6	2.30	1.8	6
P9	2.32	2.0	9
P14	2.15	1.4	14
P18	2.29	1.6	18
PD	2.21	1.8	23
P26	2.22	2.0	26
P38	2.25	2.1	38
β-$Fe_3(P_2O_7)_2$	1.33	1.2	33

The Mössbauer spectra of the precursors have been fitted with two ferric doublets [Fe(1) and Fe(2)] and two ferrous doublets [Fe(3) and Fe(4)] (Fig. 1, Table 2). Since the precursors were all amorphous it was difficult to attribute these doublets. The relatively large difference in magnitude of the quadrupolar splittings of the two ferrous cations revealed a less symmetric environment for the ferrous cations occupying the Fe(4) sites. The Mössbauer spectrum of the PD precursor was similar to those of the other precursors. Presumably the dehydration of the vivianite did not modify the nature or the distribution of the elemental clusters in the solid.

The precursors underwent a total transformation under the conditions of catalysis, leading to crystallized solids as previously described (4). X-ray diffraction patterns of the solids showed that they contained $Fe_2(PO_3OH)P_2O_7$ as the major phase along with β-$Fe_3(P_2O_7)_2$ in most of the samples; in a few cases, α-$Fe_3(P_2O_7)_2$ was present (Fig. 2). The Mössbauer spectra of the solids, presented in Fig. 3, have been fitted with an intense ferric doublet (Fe(1) attributed to $Fe_2(PO_3OH)P_2O_7$ (Table 3). Besides this doublet three ferrous doublets were not observed in all samples. The first one, Fe(2), was attributed to a ferrous site present in the amorphous phase formed at the surface of $Fe_2(PO_3OH)P_2O_7$ (4). The second one, Fe(4), characterized by a large quadrupolar splitting ($\Delta = 4.35$ mm s^{-1}), was attributed to β-$Fe_3(P_2O_7)_2$, whereas the third one, Fe(5), was attributed to α-$Fe_3(P_2O_7)_2$. These attributions were made in view of the data reported in the literature (5, 8, 15, 16). The ferric site corresponding to β-$Fe_3(P_2O_7)_2$, Fe(3), has been identified in most of the catalysts when the corresponding ferrous site was detected; however, it was absent

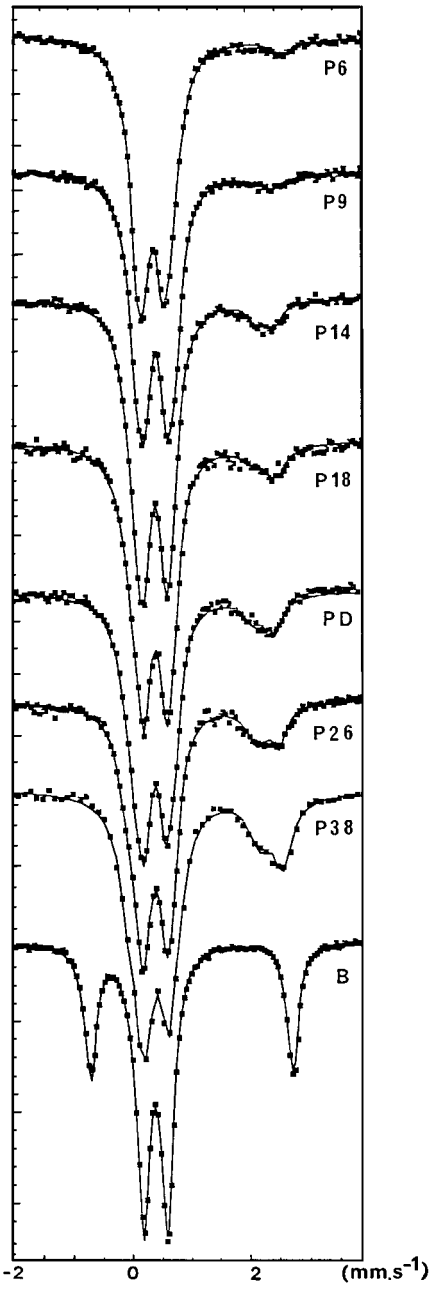

FIG. 1. Experimental Mössbauer spectra of the precursors, recorded before catalysis at 295 K. Solid lines are derived from least-squares fits.

in some cases. Furthermore, the ferric site, corresponding to α-$Fe_3(P_2O_7)_2$, was never indentified. These results are explained by the fact that the Mössbauer parameters of these ferric sites were close to those of the ferric site of $Fe_2(PO_3OH)P_2O_7$ which enable us to differentiate them. It may be noted in these cases that the linewidth of the doublet corresponding to the common ferric site was larger than that of the other doublets.

Comparison of the characterization of the solids before and after catalysis showed that the β-$Fe_3(P_2O_7)_2$ content of the catalysts increased with the reduction level of the precursors (Tables 2 and 3). Moreover, it can be seen that this content could be directly related to the presence of the ferrous site Fe(4) in the precursors before catalysis (Fig. 4). The structure of β-$Fe_3(P_2O_7)_2$ is very particular compared with other iron phosphates (8). It is built up like β-$Fe_3(P_2O_7)_2$ from $(Fe_3O_{12})^{16-}$ clusters connected to each other via P_2O_7 groups, but with clusters composed of two octahedra sharing faces with a central trigonal prism rather than three octhaedra sharing faces (Fig. 5) (8). This coordination for the central ferrous cation is rather unusual and may explain the very large quadrupolar splitting observed for this cation. The formation of such clusters could be related to the presence of Fe^{2+} in the solid before catalysis, with a distorted environment which acts as a precursor for the central atom of these clusters.

TABLE 2

Mössbauer Parameters Computed from the Spectra of the Precursors and β-$Fe_3(P_2O_7)_2$, Recorded at 295 K

Compound	Site	δ^a (mm s^{-1})	W (mm s^{-1})	Δ (mm s^{-1})	Relative intensity (%)
P6	$Fe^{3+}(1)$	0.44	0.33	0.34	61
	$Fe^{3+}(2)$	0.45	0.30	0.61	33
	$Fe^{2+}(3)$	1.19	0.26	1.83	2
	$Fe^{2+}(4)$	1.23	0.30	2.82	4
P9	$Fe^{3+}(1)$	0.43	0.31	0.36	63
	$Fe^{3+}(2)$	0.46	0.28	0.67	27
	$Fe^{2+}(3)$	1.16	0.25	1.98	3
	$Fe^{2+}(4)$	1.24	0.44	2.62	6
P14	$Fe^{3+}(1)$	0.43	0.31	0.40	65
	$Fe^{3+}(2)$	0.43	0.27	0.68	20
	$Fe^{2+}(3)$	1.28	0.28	1.82	4
	$Fe^{2+}(4)$	1.21	0.30	2.57	11
P18	$Fe^{3+}(1)$	0.44	0.33	0.39	67
	$Fe^{3+}(2)$	0.43	0.25	0.69	14
	$Fe^{2+}(3)$	1.25	0.46	1.76	6
	$Fe^{2+}(4)$	1.23	0.43	2.62	12
PD	$Fe^{3+}(1)$	0.45	0.26	0.65	56
	$Fe^{3+}(2)$	0.44	0.32	0.35	21
	$Fe^{2+}(3)$	1.10	0.51	2.15	13
	$Fe^{2+}(4)$	1.22	0.32	2.57	10
P26	$Fe^{3+}(1)$	0.43	0.31	0.36	63
	$Fe^{3+}(2)$	0.43	0.28	0.67	11
	$Fe^{2+}(3)$	1.27	0.46	1.87	16
	$Fe^{2+}(4)$	1.23	0.28	2.71	10
P38	$Fe^{3+}(1)$	0.44	0.36	0.46	62
	$Fe^{2+}(3)$	1.27	0.42	1.83	18
	$Fe^{2+}(4)$	1.29	0.35	2.65	20
β-$Fe_3(P_2O_7)_2$	Fe^{3+}	0.47	0.26	0.26	67
	Fe^{2+}	1.13	0.24	4.19	33

[a] δ, isomer shift (given with respect to α-Fe); W, linewidth; Δ, quadrupolar splitting.

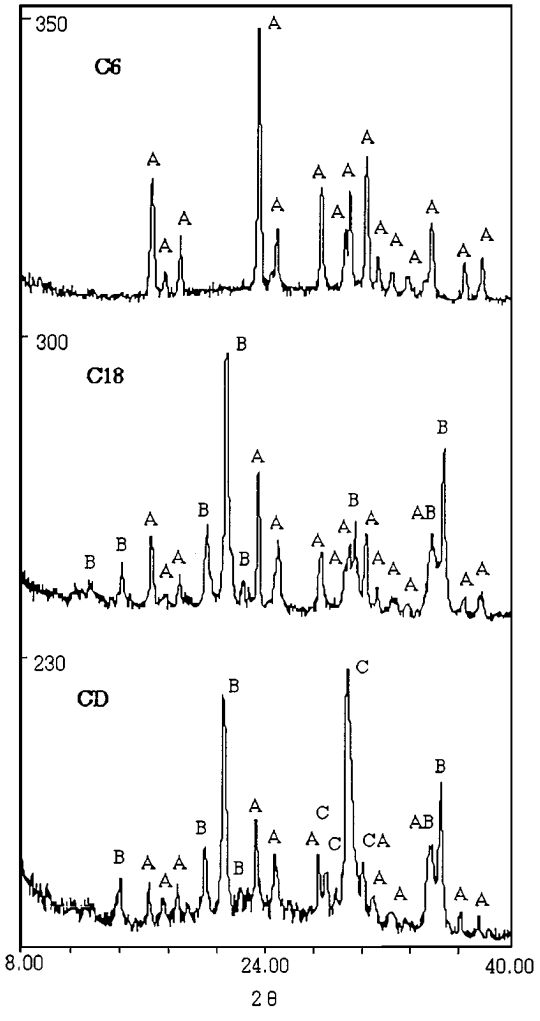

FIG. 2. X-ray diffraction patterns of catalysts containing only the phase $Fe_2(PO_3OH)P_2O_7$ (A), like C6, or in mixtures with β-$Fe_3(P_2O_7)_2$ (B) and α-$Fe_3(P_2O_7)_2$ (C), like C18 and CD.

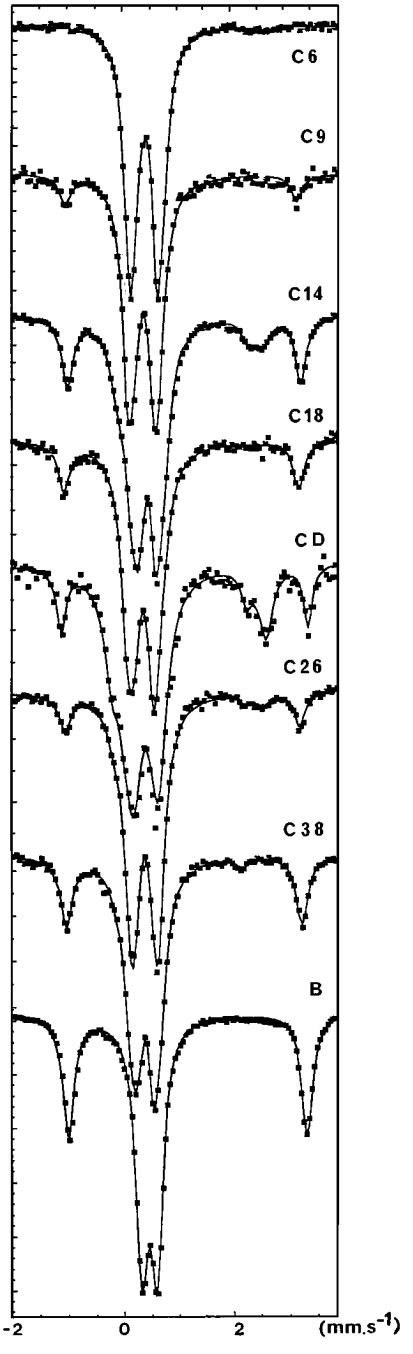

FIG. 3. Experimental Mössbauer spectra of the catalysts, recorded after catalysis at 295 K. Solid lines are derived from least-squares fits.

The pure phase β-$Fe_3(P_2O_7)_2$ was prepared as described under Experimental. The P/Fe and $Fe^{3+}/(Fe^{3+}+Fe^{2+})$ ratios of the obtained solid were in good agreement with the phase formula (Table 1). Its X-ray diffraction pattern confirmed its monophasic nature (Fig. 6). The Mössbauer spectrum of the solid (Fig. 1) was fitted with two doublets, one ferrous and one ferric, in a 2 : 1 ratio as described in the literature (Table 2) (8). Characterization of β-$Fe_3(P_2O_7)_2$ after catalytic testing by X-ray diffraction and Mössbauer spectroscopy showed that this phase has not undergone any transformation. The Mössbauer parameters were the same as those calculated before catalysis (Table 3).

3.2. Catalytic Properties of β-$Fe_3(P_2O_7)_2$-Containing Catalysts

The precursors and β-$Fe_3(P_2O_7)_2$ have been tested as catalysts under the conditions described under Experimental. The results of the catalytic tests of the solids are presented in Table 4. The catalytic properties of the catalysts were comparable except those of the β-$Fe_3(P_2O_7)_2$ phase, which was poorly active compared with the precursors and with most of the iron phosphate-based catalysts tested before (14, 15). It was also not very selective in MAA to the benefit of acetone.

TABLE 3

Mössbauer Parameters Computed from the Spectra of the Catalysts after Catalytic Tests, Recorded at 295 K

Compound	Site	δ^a (mm s^{-1})	W (mm s^{-1})	Δ (mm s^{-1})	Relative intensity (%)	Phase attribution
C6	$Fe^{3+}(1)$	0.44	0.28	0.51	98	A[b]
	$Fe^{2+}(2)$	1.19	0.26	2.37	2	A
C9	$Fe^{3+}(1)$	0.42	0.26	0.52	73	A
	$Fe^{2+}(2)$	1.13	0.28	2.33	2	A
	$Fe^{3+}(3)$	0.44	0.26	0.29	17	B
	$Fe^{2+}(4)$	1.14	0.27	4.29	8	B
C14	$Fe^{3+}(1)$	0.44	0.31	0.56	41	A + C
	$Fe^{2+}(2)$	1.13	0.28	2.33	6	A
	$Fe^{3+}(3)$	0.45	0.29	0.29	32	B
	$Fe^{2+}(4)$	1.14	0.23	4.33	14	B
	$Fe^{2+}(5)$	1.21	0.28	2.70	7	C
C18	$Fe^{3+}(1)$	0.44	0.32	0.51	66	A
	$Fe^{3+}(3)$	0.46	0.24	0.30	22	B
	$Fe^{2+}(4)$	1.15	0.24	4.34	12	B
CD	$Fe^{3+}(1)$	0.46	0.42	0.47	68	A + B + C
	$Fe^{2+}(2)$	1.22	0.24	2.35	3	A
	$Fe^{2+}(4)$	1.23	0.22	4.60	10	B
	$Fe^{2+}(5)$	1.29	0.30	2.88	19	C
C26	$Fe^{3+}(1)$	0.44	0.34	0.45	85	A + B + C
	$Fe^{2+}(2)$	1.19	0.26	2.30	3	A
	$Fe^{2+}(4)$	1.16	0.24	4.35	9	B
	$Fe^{2+}(5)$	1.24	0.23	2.79	3	C
C38	$Fe^{3+}(1)$	0.44	0.31	0.52	40	A
	$Fe^{2+}(2)$	1.10	0.28	2.35	2	A
	$Fe^{3+}(3)$	0.46	0.28	0.30	39	B
	$Fe^{2+}(4)$	1.18	0.25	4.36	19	B
β-$Fe_3(P_2O_7)_2$	$Fe^{3+}(3)$	0.46	0.27	0.27	68	B
	$Fe^{2+}(4)$	1.15	0.24	4.27	32	B

[a] δ, isomer shift (given with respect to α-Fe); W, linewidth; Δ, quadrupolar splitting.
[b] (A) $Fe_2(PO_3OH)P_2O_7$, (B) β-$Fe_3(P_2O_7)_2$, (C) α-$Fe_3(P_2O_7)_2$.

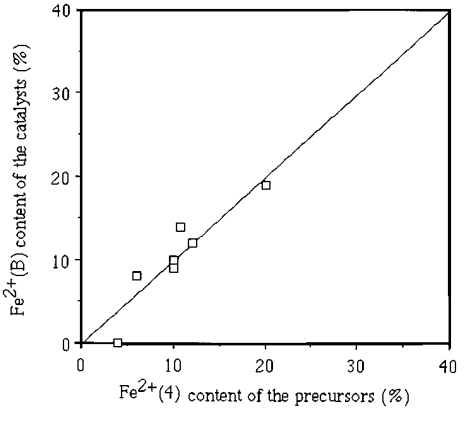

FIG. 4. Relative content of Fe^{2+} corresponding to β-$Fe_3(P_2O_7)_2$ [Fe^{2+}(B)] versus the relative content of Fe^{2+}(4) present in the precursors.

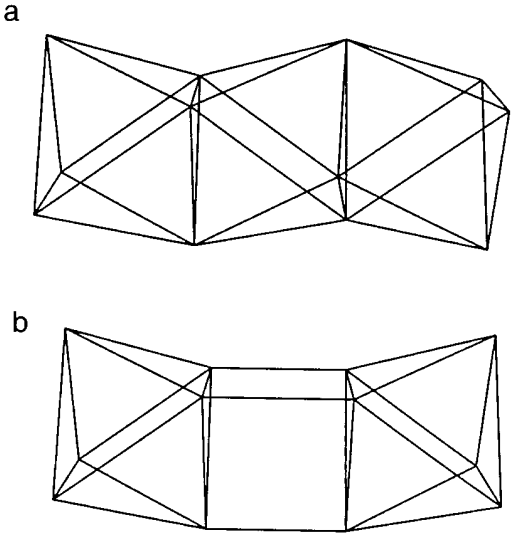

FIG. 5. Schematic representation of the two types of Fe_3O_{12} clusters in the structures of α-$Fe_3(P_2O_7)_2$ (a) and β-$Fe_3(P_2O_7)_2$ (b).

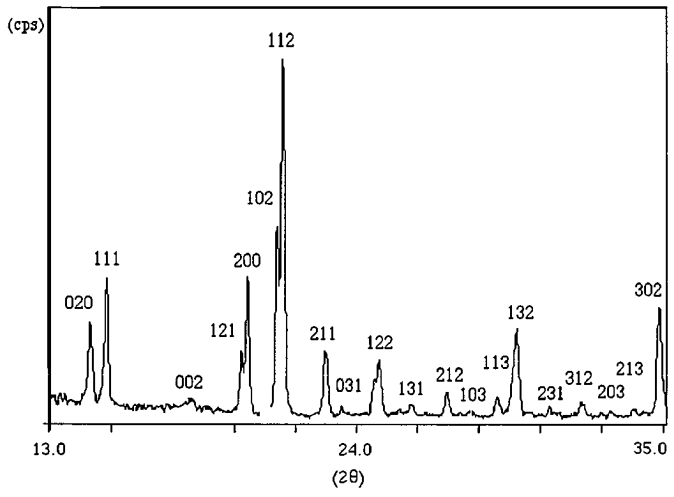

FIG. 6. Indexed X-ray diffraction pattern of the synthesized β-$Fe_3(P_2O_7)_2$ phase.

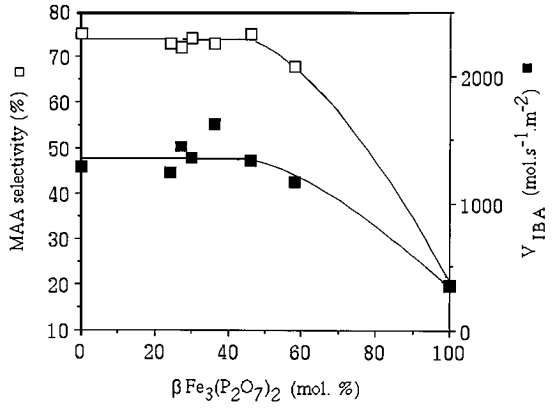

FIG. 7. Rate of transformation of IBA and selectivity in MAA as a function of the molar percentage of β-$Fe_3(P_2O_7)_2$ in the catalysts.

The rate of transformation of IBA and the selectivity in MAA observed on the different catalysts were plotted as a function of their β-$Fe_3(P_2O_7)_2$ content after catalysis (Fig. 7). The activities and selectivities for MAA remained almost unchanged for catalysts containing up to 50 mol% β-$Fe_3(P_2O_7)_2$ and decreased at higher contents. Taking into account that the surface areas of samples were approximately the same, this result may be explained only by the fact that the β-$Fe_3(P_2O_7)_2$ phase was preferentially located inside the grains and thus did not influence the catalytic properties of the solids before it reached an amount such that it appeared as an independent phase. Since β-$Fe_3(P_2O_7)_2$ was almost inactive and poorly selective, the catalytic properties of the catalysts decreased rapidly. This is compatible with the structural origin of the β-$Fe_3(P_2O_7)_2$ phase. If this reduced phase was formed under the conditions of the catalytic run it would have been at the surface of the catalyst grains and would have had an effect at low concentration. It was observed that β-$Fe_3(P_2O_7)_2$ did not undergo any transformation under catalytic conditions. The trigonal prismatic coordination of the Fe^{2+} seems to inhibit it from undergoing any oxidation, as is the case when Fe^{2+} occupies an octahedron sharing faces with one or two other octahedra (4, 6). This may explain the low catalytic activity of this phase. This observation correlates with a theoretical study of clusters of face-sharing FeO_6 octahedra which has recently shown that an electronic delocalization between two adjacent iron cations in a Fe_3O_{12} cluster could take place very easily when the central element is an octahedron, but is almost impossible when it is a trigonal prism (17).

3.3. *Catalytic Properties of α-$Fe_3(P_2O_7)_2$-Containing Catalysts*

Two precursors (C14 and C26) were tested before recovery under less oxidizing conditions. A comparison of their phase compositions, calculated from Mössbauer data, is presented in Table 5. The catalysts were composed of various amounts of α-$Fe_3(P_2O_7)_2$, but approximately the

TABLE 4

Catalytic Data of the Precursors at 658 K in the Oxidative Dehydrogenation of Isobutyric Acid

Catalyst	Selectivity (%)				Rate of formation of MAA (10^{-8} mol s^{-1} m^{-2})
	CO_2	PRO[a]	ACE	MAA	
C6	2	9	14	75	960
C9	1	10	16	73	900
C14	1	8	15	75	1000
C18	2	8	16	73	1190
CD	2	9	16	74	1180
C26	4	8	16	72	1040
C38	4	8	20	68	790
β-$Fe_3(P_2O_7)_2$	49	3	8	20	69

[a] PRO, propene; ACE, acetone; MAA, methacrylic acid.

TABLE 5

Fe^{2+} Content of the Phase $Fe_2(PO_3OH)P_2O_7$ and Phase Composition of the Catalysts, Calculated from Mössbauer Data, as a Function of the Partial Pressure of Oxygen Used for the Test When the Catalysts Have Been Recovered

Catalyst	Fe^{2+}(2) (%)	Molar phase composition (%)				O_2 partial pressure (kPa)
		A[a]	B	C	B′	
C18	<1	73	27	—	27	4.26
C26	5	72	21	7	22	2.63
C14	18	48	35	17	28	1.32

[a] (A) $Fe_2(PO_3OH)P_2O_7$; (B) β-$Fe_3(P_2O_7)_2$; (C) α-$Fe_3(P_2O_7)_2$; (B′) β-$Fe_3(P_2O_7)_2$ phase content evaluated from the Fe(3) content of the precursor.

same amount of β-$Fe_3(P_2O_7)_2$. The precursors tested under less oxidizing conditions appeared more reduced. Both the reduction level of the phase $Fe_2(PO_3OH)P_2O_7$ and the mixed valence phase α-$Fe_3(P_2O_7)_2$ content increased when the oxygen partial pressure decreased. The presence of α-$Fe_3(P_2O_7)_2$ was also confirmed by X-ray diffraction (Fig. 2). Overall, the oxidoreduction conditions did not seem to influence β-$Fe_3(P_2O_7)_2$ content; only a small increase in phase content was observed at the lower oxygen partial pressure (Table 5), reinforcing our hypothesis concerning the conditions of formation of this phase. This has been shown by comparing the amount of β-$Fe_3(P_2O_7)_2$ phase calculated from Mössbauer data (B) and that evaluated from the Fe(3) content of the catalyst precursors (B′). The phase α-$Fe_3(P_2O_7)_2$ was also detected in large quantity in the catalyst obtained after catalytic testing of the precursor prepared with dehydrated vivianite (CD) (Table 3). This result showed that the water in the precursors has an important role in the formation of PO_3OH groups in the catalysts and in the crystallization of the hydrated $Fe_2(PO_3OH)P_2O_7$ phase. The water in the precursor should also play a role in avoiding a too high reduction leading to the formation of the more reduced phase α-$Fe_3(P_2O_7)_2$. Previous studies have shown that the reduction of $Fe_2(PO_3OH)P_2O_7$ took place at its surface and was related to the presence of an amorphous phase covering the particles of $Fe_2(PO_3OH)P_2O_7$ (4). The results obtained showed that the reduction level of this phase never exceeded 6 to 7% and that all further oxidation of the catalysts led to an increase in the phase content in α-$Fe_3(P_2O_7)_2$. It is proposed that the oxidation level of the amorphous phase may present an upper limit at which the α-$Fe_3(P_2O_7)_2$ phase crystallized.

To study the effect of the presence of α-$Fe_3(P_2O_7)_2$ on the catalytic properties of the catalysts, we have gathered in Table 6 the catalytic data obtained with two catalysts that contained the same amount of β-$Fe_3(P_2O_7)_2$ plus in one case mainly α-$Fe_3(P_2O_7)_2$ and in the other, $Fe_2(PO_3OH)P_2O_7$. The catalytic properties of these two last phases appeared very close. This result confirmed the similarities observed when the catalytic properties of $Fe_2(PO_3OH)P_2O_7$ and an industrial catalyst (the active phase of which was α-$Fe_3(P_2O_7)_2$) were compared (4). The amorphous phase

TABLE 6

Comparison of the Catalytic Properties of the Catalysts C18 and CD as a Function of Their Phase Composition

	Molar phase composition (%)			MAA selectivity	Rate of formation of MAA
Catalyst	A[a]	B	C	(%)	(10^{-8} mol s^{-1} m^{-2})
C18	73	27	0	73	1190
CD	17	29	54	74	1180

[a] (A) $Fe_2(PO_3OH)P_2O_7$; (B) β-$Fe_3(P_2O_7)_2$; (C) α-$Fe_3(P_2O_7)_2$.

on the $Fe_2(PO_3OH)P_2O_7$ particles should contain the same species as in the bulk: PO_3OH and P_2O_7 groups and Fe_2O_9 clusters (8). It has previously been proposed that the α-$Fe_3(P_2O_7)_2$ phase is superficially oxidized and hydrated and thus has at its surface PO_3OH, PO_4, and P_2O_7 groups and Fe_3O_{12} clusters (18). Both phases have the same species at their surface and this may explain the similarities observed in their catalytic properties. It may be proposed that Fe_3O_{12} instead of Fe_2O_9 was also formed on reduction at the surface of the $Fe_2(PO_3OH)P_2O_7$ phase. Experimentally it has been observed that phases containing dimeric clusters ($Fe_2O_6OH_3$) like $Fe_4(PO_4)_3(OH)_3$ are not very active compared with phases of the same type like $Fe_3(PO_4)_2(OH)_2$, which contained trimeric clusters ($Fe_3O_8OH_4$) (18). From a theoretical point of view there is also a great difference in electron localization in the clusters. In the trimers the electrons can be delocalized between the central and one of the terminal sites, whereas in dimers the excess electrons should be localized at one site (17, 19).

4. CONCLUSION

The results described in this paper show that the high-temperature phase β-$Fe_3(P_2O_7)_2$ can be obtained at only 658 K under the conditions of catalytic run, in the catalysts prepared by refluxing vivianite and pyrophosphoric acid in acetone. The amount of this phase has been related to the amount in the precursors of the catalysts of a ferrous cation with a distorted octahedral environment. This leads us to propose that the presence of β-$Fe_3(P_2O_7)_2$ in the catalysts was related to the structure and reduction level of the precursors. Clusters (Fe_3O_{12}) specific to the structure of the β-$Fe_3(P_2O_7)_2$ phase, in which the central ferrous cation has a trigonal prismatic coordination, may be formed from ferrous cations having a distorted environment in the amorphous precursors. From a catalytic point of view the β-$Fe_3(P_2O_7)_2$ phase appeared to be both poorly active and selective and no synergy effect seemed to take place between this phase and the $Fe_2(PO_3OH)P_2O_7$ phase.

When precursors were tested under low oxygen partial pressure, it was observed that the phase α-$Fe_3(P_2O_7)_2$ was formed. The amount of this phase increased when the oxygen partial pressure decreased, in the same time the $Fe_2(PO_3OH)P_2O_7$ phase was superficially more reduced. If the formation of α-$Fe_3(P_2O_7)_2$ depends mainly on the conditions of catalytic test, it may also be related to the method of preparation of the catalysts, since catalysts prepared with dehydrated vivianite exhibit large amounts of α-$Fe_3(P_2O_7)_2$. Comparison of the catalytic properties of the α-$Fe_3(P_2O_7)_2$ and $Fe_2(PO_3OH)P_2O_7$ phases showed that they yield performance catalysts with very close catalytic properties. This strongly suggests that the two phases have at the surface the same species and reinforces the hypothesis made on the role of water on the catalysts allowing stabilization of

PO_3OH groups at the surface and on the nature of the best catalytic sites corresponding to Fe_3O_{12} clusters.

REFERENCES

1. Cavaterra, E., *et al.*, French Patent 2 245 604 assigned to Montedison (1974).
2. Statz, R. J., *et al.,* U.S. Patent 4 232 174 assigned to Dupont de Nemours (1980).
3. Daniel, C., U.S. Patent 4 410 727 assigned to Ashland Oil Inc. (1983).
4. Bonnet, P., Millet, J. M. M., Leclerc, C., and Vedrine, J. C., *J. Catal.*
5. Millet, J. M. M., Vedrine, J. C., and Hecquet, G., *Stud. Surf. Sci. Catal.* **55**, 833 (1990).
6. Millet, J. M. M., Thesis, Lyon, No. 259-90 (1990).
7. Védrine, J. C., Auroux, A., Coudurier, G., and Millet, J. M. M., "Catalisis y Quimica Fina, Anales del Grupo Especializado de Catalisis," Series: Actas No. 16, Vol. 5, p. 237. Servicio de publicaciones de la Universidad de Cordoba, Cordoba, 1993.
8. Ijjaali, M., Venturini, Gerardin, R., Malaman, B., and Gleitzer, C., *Eur. J. Solid State Inorg. Chem.* **28**, 983 (1991).
9. Muneyama, E., Kunishige, A., Ohdan, K., and Ai, M., *Appl. Catal. A* **116**, 165 (1994).
10. Muneyama, E., Kunishige, A., Ohdan, K., and Ai, M., *J. Mol. Catal.* **89**, 371 (1994).
11. Millet, J. M. M., and Védrine, J. C., *Appl. Catal.* **76**, 209 (1991).
12. Millet, J. M. M., Virely, C., Forissier, M., Bussière, P., and Védrine, J. C., *Hyperfine Interact.* **46**, 619 (1989).
13. Virely, C., Fabregue, O., and Forissier, M., *Bull. Soc. Chim.* **3**, 457 (1988).
14. Virely, C., Forrissier, M., Millet, J. M. M., and Vedrine, J. C., *J. Mol. Catal.* **71**, 199 (1992).
15. Rouzies, D., Millet, J. M. M., Siew Hew Sam, D., and Vedrine, J. C., *Appl. Catal.* **124**, 198 (1995).
16. Reiff, W. M., and Torardi, C. C., *Hyperfine Interact.* **53**, 403 (1990).
17. Robert, V., Borshch, S. A., and Bigot, B., *J. Phys. Chem.* **100**(2), (1996).
18. Millet, J. M. M., Rouzies, D., and Védrine, J. C., *Appl. Catal.* **124**, 205 (1995).
19. Robert, V., Borshch, S. A., Bigot, B., *Chem. Phys. Lett.* **236**, 491 (1995).